Journal of Magnetic Resonance 197 (2009) 40–47

Contents lists available at ScienceDirect

Journal of Magnetic Resonance

journal homepage: www.elsevier.com/locate/jmr

In vitro determination of biomechanical properties of human articular cartilage in osteoarthritis using multi-parametric MRI

Vladimir Juras [a,b,e,*], Michal Bittsansky [a], Zuzana Majdisova [a,b,e], Pavol Szomolanyi [a,b,e], Irene Sulzbacher [c], Stefan Gäbler [d], Jürgen Stampfl [d], Georg Schüller [e,f], Siegfried Trattnig [a,e]

[a] MR Center, Highfield MR, Department of Radiology, Medical University of Vienna, Lazarettgasse 14, 1090 Vienna, Austria
[b] Department of Imaging Methods, Institute of Measurement Science, Slovak Academy of Sciences, Dubravska cesta 9, 84104 Bratislava, Slovakia
[c] Clinical Institute of Pathology, Medical University of Vienna, Waehringer Guertel 18-20, 1090 Vienna, Austria
[d] TU Wien, Institute of Materials Science and Technology, Favoritenstraße 9-11, 1040 Vienna, Austria
[e] Austrian Cluster for Tissue Regeneration, Donaueschingenstrasse 13, A-1200 Vienna, Austria
[f] Ludwig Boltzmann Institute for Experimental and Clinical Traumatology, Donaueschingenstr. 13, A-1200 Vienna, Austria

ARTICLE INFO

Article history:
Received 24 June 2008
Revised 20 November 2008
Available online 8 December 2008

Keywords:
Cartilage
MRI
dGEMRIC
T_2 relaxometry
Diffusion
Biomechanical parameters
Osteoarthritis

ABSTRACT

The objective of this study was to evaluate the correlations between MR parameters and the biomechanical properties of naturally degenerated human articular cartilage. Human cartilage explants from the femoral condyles of patients who underwent total knee replacement were evaluated on a micro-imaging system at 3 T. To quantify glycosaminoglycan (GAG) content, delayed gadolinium-enhanced MRI of the cartilage (dGEMRIC) was used. T_2 maps were created by using multi-echo, multi-slice spin echo sequences with six echoes: 15, 30, 45, 60, 75, and 90 ms. Data for apparent diffusion constant (ADC) maps were obtained from pulsed gradient spin echo (PGSE) sequences with five *b*-values: 10.472, 220.0, 627.0, 452.8, 724.5, and 957.7. MR parameters were correlated with mechanical parameters (instantaneous (I) and equilibrium (Eq) modulus and relaxation time (τ)), and the OA stage of each cartilage specimen was determined by histological evaluation of hematoxylin–eosin stained slices. For some parameters, a high correlation was found: the correlation of T_{1Gd} vs Eq ($r = 0.8095$), T_{1Gd} vs I/Eq ($r = -0.8441$) and T_{1Gd} vs τ ($r = 0.8469$). The correlation of T_2 and ADC with selected biomechanical parameters was not statistically significant.

In conclusion, GAG content measured by dGEMRIC is highly related to the selected biomechanical properties of naturally degenerated articular cartilage. In contrast, T_2 and ADC were unable to estimate these properties. The results of the study imply that some MR parameters can non-invasively predict the biomechanical properties of degenerated articular cartilage.

1. Introduction

The articular cartilage can be thought of as a fiber-reinforced anisotropic composite material. The mechanical properties of articular cartilage are a function of the essential mechanical properties of the tissue components and the interplay of these components during loading. Articular cartilage is a bi-phasic material: the permeable solid section is represented by a solid matrix that consists of collagen fibers and proteoglycan molecules, and the fluid section is composed of extracellular water with dissolved ions and nutrients. Most of the fluid can move through the collagen network during loading. Experimental data from articular cartilage can be assessed by single-, bi- or multi-phasic models [1–4].

The mechanical properties of articular cartilage arise from the complex structure and interactions of its biochemical constituents: mostly water, electrolytes, and a solid matrix composed primarily of collagen and proteoglycan. Laasanen et al. showed that collagen primarily controls the dynamic tissue response while proteoglycans affect more the static properties [5]. In the ex-vivo study published by Appleyard et al. there was found a strong and significant correlation between shear modulus and collagen content, whereas correlation between shear modulus and water content was not significant [6]. Stiffness and strength of articular cartilage tissue depended on the density and orientation of collagen fibers, and the type or amount of collagen cross-linking [7].

Various imaging methods have been applied to assess articular cartilage. These include standard radiography [8], CT arthrography [9], ultrasonography [10], and MR imaging [11,12]. MRI offers excellent soft tissue contrast and multi-planar imaging capability, and therefore, it has become the method of choice to diagnose

* Corresponding author. Address: MR Center, Highfield MR, Department of Radiology, Medical University of Vienna, Lazarettgasse 14, 1090 Vienna, Austria. Fax: +43 1 40400 7631.
E-mail address: vladimir.juras@meduniwien.ac.at (V. Juras).

1090-7807/$ - see front matter © 2009 Published by Elsevier Inc.
doi:10.1016/j.jmr.2008.11.019

cartilage diseases. It also provides valuable information on composition and structural changes in cartilage. For determination of glycosaminoglycan (GAG) content, delayed gadolinium-enhanced MRI of cartilage (dGEMRIC) was developed and has been used to answer clinical questions [13,14]. Since transversal relaxation time, T_2, is related to collagen matrix composition and is primarily influenced by collagen fiber orientation [15] and water content [16], T_2 has been successfully used for *in vitro* [17] and *in vivo* [18,19] cartilage tissue assessment. Another useful parameter that reflects the functional properties of cartilage tissue is diffusivity. The idea of using gradients to make the MR imaging signal sensitive to the molecular motion of water was introduced by Stejskal and Tanner in 1965 [20], and currently, there are a few sequences based on diffusion weighting that have been successfully used for evaluation of cartilage function and its structure [21–24].

The mechanical properties of articular cartilage can be evaluated on different levels, from an *in vivo* investigation of intact joints by indentation [25] to *in vitro* studies of explants [26] and to cellular and molecular levels [26]. For viscoelastic materials like cartilage, two biomechanical parameters play a role: firstly the instantaneous modulus (*I*), which describes the initial stiffness upon loading, and secondly the equilibrium modulus (*Eq*) which describes only the time independent share of the stiffness. The ratio between *I* and *Eq* gives a measure of the viscoelastic character. If *I*/*Eq* is close to unity the material is merely elastic, and is better termed spontaneous elastic. If *I*/*Eq* is greater than two, the material is strongly viscoelastic. For cartilage it may be said that the smaller *I*/*Eq* the more vital is the cartilage, which means it is able to better withstand static loading (carrying heavy loads for instance) as well as fast and extremely high load cycles (from jumping or running for instance). The mechanical properties of cartilage tissue are strongly related to the OA stage of cartilage [27]. Changes in the biomechanical properties of articular cartilage are one of the first signs of the tissue degeneration. For cartilage degeneration, it is necessary to know how cartilage maintains its functionality and how cartilage responds to the ever-changing mechanical environment. The biomechanical properties of articular cartilage can be assessed relatively precisely, however, ex-vivo [28] or invasively during an arthroscopic procedure [29]. MRI provides the possibility to non-invasively assess the biomechanical properties of articular cartilage provides MRI. In the past, several studies suggested the way how MRI parameters might be used for biomechanical parameters assessment [28,30,31]. However, to the best of our knowledge, the correlation between biomechanical properties and MR parameters of degenerated human articular cartilage stages has not been previously determined.

Therefore, in the presented study we hypothesized that biochemical parameters derived non-invasively from MRI as a non-invasive imaging method can predict the biomechanical properties of naturally degenerated human articular cartilage. Thus the aim of this work was to determine the correlation of MR relaxation times and diffusion constants at 3 T with an instantaneous and an equilibrium modulus.

2. Materials and methods

2.1. Sample preparation

Bone-cartilage specimens from patients who underwent total knee replacement surgery in an orthopedic hospital were delivered to our laboratory, several hours after surgery, in a frozen state. Thirteen specimens were harvested from the same site of the weight bearing area in lateral femoral condyles with different stages of osteoarthritis. Samples with extensively eroded cartilage tissue were excluded from the study. The size of the sample was chosen in order to fit into the micro-imaging device chamber; the mean size was base-x × base-y × height, 9.45 ± 1.33 × 9.81 ± 3.65 × 5.69 ± 1.41 (in mm). Mean cartilage thickness was 1.8 ± 0.33 mm. Each sample was immediately stored in the freezer at −18 °C for 48 h. Approximately 6 h before MR examination, the sample was thawed at room temperature and secured in a waterproof chamber.

2.2. MRI examinations

MRI exams were performed on a Bruker 3T Medspec whole-body scanner (Bruker, Ettlingen, Germany) equipped with a micro-imaging gradient insert BGA 12 (Bruker, Ettlingen, Germany). The micro-imaging gradient system was capable of delivering 200 mT/m. A 35 mm inner diameter resonator was used. The cartilage samples were placed in waterproof chamber filled with PBS (Phosphate Buffer Saline), with the cartilage surface perpendicular to the static magnetic field. All MR measurements were performed at 12 °C.

For mapping of longitudinal relaxation time (T_1), a spin echo pulse sequence with inversion recovery (IR) was used. A T_1 map was calculated from six different sequential scans with inversion times (*TI*) of 15, 30, 60, 160, 400, and 2000 ms, each with an echo time (*TE*) of 15 ms. To ensure equal time for longitudinal relaxation at different inversion times relaxation delay (*RD*) was added to *TR* 4000 ms. T_1 maps were constructed by nonlinear numerical fitting of absolute MR signal intensity values according to the function, $S(TI) = \mid S(0) \times (1 - 2e^{-TI/T_1}) \mid$, which describes T_1 relaxation using the IR sequence. Scans were performed first in the pre-contrast conditions (cartilage sample soaked in PBS), and subsequently after adding contrast agent (1 mM solution of Gd-DTPA^{2-} (Gadolinium DiethyleneTriaminePentaacetic Acid)) in order to calculate Gd-DTPA^{2-} concentration using the following expression:

$$[\text{Gd-DTPA}] = 1/R(1/T_{1\text{Gd}} - 1/T_1) \quad (1)$$

assuming that the relaxivity (R) of Gd-DTPA^{2-} is the same as in saline at 37 °C, R = 3.1 ± 0.3 L mM^{-1} s^{-1} at 3 T [32]. Post-contrast measurements were performed after 16 h after contrast media addition to allow full equilibrium.

A multi-echo, multi-slice spin echo sequence was used for transversal relaxation time (T_2) map construction with six different *TE*s: 15, 30, 45, 60, 75, and 90 ms. From the acquired data, a pixel-by-pixel basis fitting of signal intensities according to the function, $S(TE) = S(0) \times e^{-TE/T_2}$, was performed. *TR* was 4000 ms and six averages were used.

A pulsed gradient spin echo (PGSE) sequence was used for ADC (Apparent Diffusion Constant) map construction [33] with following parameters were used: time between diffusion gradients leading edges, 16.26 ms; duration of diffusion gradients, 5 ms; amplitude of the gradient pulses (5, 80, 120, 155, and 180); and corresponding *b*-values were: *b* (10.472, 220.627, 452.8, 724.5, and 957.7). A pixel-by-pixel basis fitting of signal intensities according to the function $S(t) = S(0) \times e^{-bD}$ was performed. A *TR* of 4000 ms with six averages was used. Diffusion gradients were in the direction of the read-out gradient, i.e., from subchondral bone toward the cartilage surface.

For T_1, T_2, and ADC mapping the following parameters were used: acquisition matrix, 128 × 96; reconstructed image matrix, 128 × 128; FOV, 30 × 30 mm; and bandwidth, 15 kHz. Total measuring times were: 4 h 18 min for T_1 mapping; 38 min for T_2 mapping and 36 min for ADC mapping.

2.3. MRI data evaluation

MR parameters were evaluated with software written in IDL (Interactive Data Language, Research Systems, Inc, Boulder, CO, USA). This software allows direct comparison among all maps by simple selection of a region of interest (ROI) within the proton den-

sity (PD)-weighted image and the performance of an evaluation on all maps. ROI was selected for T_1, T_2, and ADC maps separately for each cartilage zone. Since the micro-gradient insert allows data acquisition with high in-plane resolution (234 μm), it was possible to conveniently select three different cartilage zones (superficial, middle, and deep). Based on previously published results, particular zones were selected as follows: the superficial zone was defined as approximately 16% of cartilage thickness, from the cartilage surface straight down to deeper tissue; the middle zone was defined as the zone with 31% of the cartilage, situated adjacent to the superficial zone; and the deep zone was defined as the remaining 53% of the cartilage down to the cartilage-bone interface [34]. The bulk values (across whole cartilage thickness) of MR parameters were calculated and evaluated as well.

2.4. Histology procedures

To reveal the status of each specimen, a histological section was prepared from each cartilage explant. The section was cut parallel to the imaging planes in the region of cartilage damage. The sections, measuring 3 mm, were decalcified with ethylene diamine tetraacetic acid (EDTA). Histological slides were cut on a microtome at a thickness of 3 μm and stained with hematoxylin & eosin (H&E). Histological slides were evaluated by an experienced pathologist (I.S.). Four levels of cartilage degeneration were graded, namely, 1 for healthy cartilage, 2 for mild OA (defects in the superficial zone, corresponding to Mankin score 1), 3 for moderate (superficial fissures, moderate reduction in proteoglycan (PG) content, Mankin score 2–4), and, finally, 4 for advanced OA (deep cracks, Mankin score > 4).

2.5. Mechanical testing

Macroscopic indentation tests were performed uniaxially on a Zwick Z050 universal testing device with a 20N-load cell of 1 mN resolution. The spherical indenter had a diameter of 3 mm and the cartilage surface was oriented orthogonally to the indenter in most cases. From the MRI data, the cartilage thickness was measured and the regions with the most regular cartilage thickness were selected for indentation. During mechanical testing the samples were kept hydrated by PBS airbrushing. The experimental setup for the mechanical testing is depicted in the Fig. 1. Moduli for the indentations were calculated using a common formula for cartilage Eq.(2) derived by Hayes et al. [1].

$$\kappa = \frac{F(1-\nu)}{4 r_{act} G s} \tag{2}$$

This formula was reorganized Eq.(3) and, under utilization of Eq.(4), changed to Eq.(5).

$$G = \frac{F(1-\nu)}{4 r_{act} s \kappa} \tag{3}$$

$$G = \frac{E}{(2+2\nu)} \tag{4}$$

$$E = \frac{F(1-\nu)^2}{2 r_{act} s \kappa} \tag{5}$$

where κ is a dimensionless scaling factor, F is the force in Newton, ν is the Poisson's ratio, r_{act} is the actual indenting radius of the indenter in mm, G is the shear modulus in N/mm^2, E is the Young's modulus, and s is the penetration depth. Poisson's ratio for cartilage was assumed to be 0.4, based on the literature [29,35,36] that describes apparent values between 0.35 and 0.5 for indentation, which decreases with degradation of the tissue [37]. As the Young's modulus is defined as a time-independent variable, it is not suitable for use with materials with varying stiffness, which is what most polymers are, for instance. Instantaneous and equilibrium moduli are values of Eq. (5) in specific moments. That is why E, being a function of time is generally called a "modulus" for viscoelastic materials.

Deviating from the general rule in indentation testing to restrict penetration to a maximum of 10% of the sample thickness [38], in order to securely avoid substrate influence, cartilage was squeezed 15%. This measure was taken cautiously to obtain reasonable data because of a "come-in" effect that distorts the modulus for the first tens of microns (Fig. 2). The effect occurs independent of the tested material (also for soft polymers) and pretends a massive decrease in modulus from virtually infinite values to a certain plateau, while the influence of a bony substrate would be to increase the apparent modulus. Such an influence of the substrate could only be found for real compressions of more than 20%, and would be seen in the modulus-penetration depth diagrams as a nonlinear modulus increase [39]. The relaxation time (τ) under load is defined as follows:

$$\tau = t\left(\frac{I}{e}\right) - t(I) \tag{6}$$

where I is the instantaneous modulus (taken at the local minimum of elastic modulus values upon loading), e is Euler's number, $t(I)$ is the time at which the modulus value is termed the instantaneous modulus, and $t(I/e)$ is the time at which the modulus value decreased to approximately 36.8% of its original value. Equilibrium moduli (Eq) were obtained after static loading for 30 min.

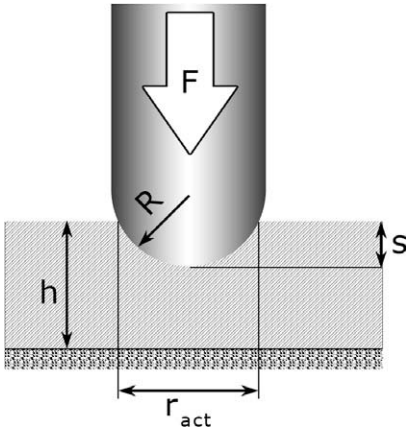

Fig. 1. Diagram of indentation test performed in order to determine the biomechanical properties of cartilage specimen; h: cartilage thickness; F: applied force; s: penetration depth; R: indenter radius; r_{act}: actual indenting radius.

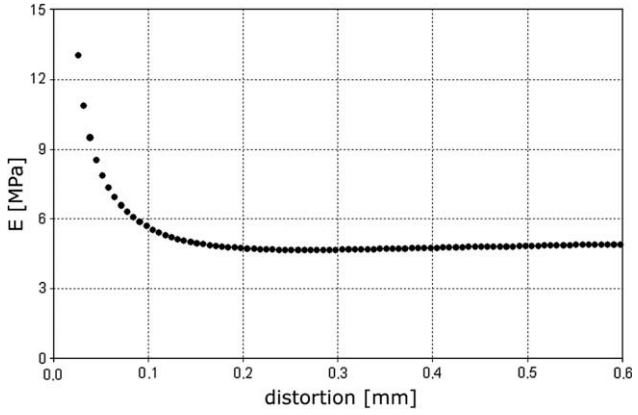

Fig. 2. Microindentation with spherical indenter of 3 mm diameter; plot of E-modulus vs distortion depicts an example of the "come-in" effect.

2.6. Statistical evaluation

Correlation coefficients between MR parameters (separately in each zone) and biomechanical parameters were calculated using a Pearson coefficient. All variables were normally distributed and were independent of each other, as assumed by a Pearson correlation calculation.

3. Results

Histological evaluation revealed seven samples with mild OA, four with moderate OA and one with advanced OA.

In the comparison between mechanical properties and MRI parameters of cartilage samples in different OA stages a high correlation for some parameters was found, e.g., the correlation between *I*/*Eq* and bulk [Gd-DTPA] ($r = 0.9320$). In general, T_{1Gd} and [Gd-DTPA] were in high correlation with the majority of the tested mechanical parameters, moreover, T_{1Gd} correlated with *Eq*, *I*/*Eq* ratio and τ in almost all layers. Correlation of [Gd-DTPA] with biomechanical parameters across particular zones was not as homogeneous as in case of T_{1Gd}—Pearson coefficients in deep and superficial zones were relatively low in comparison to middle zone and bulk values. For bulk T_2, the highest correlation was found with *Eq* ($r = 0.4717$). In general, all correlations of T_2 and biomechanical parameters, across particular cartilage zones, were lower than 0.5 Bulk ADC correlated mostly again with *Eq* ($r = -0.5236$). Highest correlation of ADC was with τ ($r = -0.7262$) in superficial zone. Figs. 3–5 depict the plots of the most striking correlations of T_{1Gd} vs *Eq*, T_{1Gd} vs τ and T_{1Gd} vs *I*/*Eq*. Pearson coefficients for particular correlations are summarized in Table 1 and MR parameters are summarized in Table 2.

In different samples, values of *I* ranged from 2.51 to 10.7 MPa (mean, 4 ± 2 MPa), and values of *Eq* ranged from 0.07 to 2.86 MPa (mean, 0.8 ± 0.9 MPa). Minimal τ was 3.8 s, and maximal was 22.6 s (mean 11 ± 4 s). The mean instantaneous and equilibrium modulus ratio was 19 ± 9.

T_{1Gd}, T_2, and ADC maps in different stages of articular cartilage degeneration are depicted in Figs. 6 and 7.

4. Discussion

This study revealed a high correlation between some quantitative MR parameters (post-contrast T_1 and contrast agent concentration) and biomechanical parameters (*Eq*, *I*/*Eq*, and τ) in naturally degenerated human articular cartilage.

It is generally accepted that the biomechanical properties of articular cartilage depend on the biochemical composition, the ultrastructural organization, and the interaction of the matrix molecules. Since alterations of the structural and biochemical properties are one of the first manifestations of articular cartilage degeneration, biomechanical properties are sensitive to pathological changes in the tissue [40]. In addition to biochemical analysis of articular cartilage components, direct mechanical testing is a very reliable indicator of the functional properties of the tissue. The mechanical testing of articular cartilage has been performed using many experimental setups, including confined and unconfined compression and indentation methods [41]. The preferred method for characterizing the degenerative state of articular cartilage has been the indentation technique [41]. Some special mechanical testing devices have been also reported in the literature [42,43]. Successive mechanical testing of articular cartilage *in vivo* during arthroscopy was introduced by Lyyra et al. [29]; however, this method has some limitations due to its invasive nature.

The values of instantaneous (*I*) and equilibrium (*E*) moduli measured in this study are in good agreement with previously published results [44]. The ratio between *I* and *Eq* reflects the measure of the viscoelastic character of articlular cartilage tissue. Since cartilages in different stages of degeneration were assessed in this study, different levels of GAG loss can be expected. The lower the *I*/*Eq* ratio is, the better the mechanical properties of cartilage are. Therefore, the results of this study indicate that GAG loss may be related to stiffness and vitality of cartilage. The resistance to deformation and fluid flow through the tissue depends on the amount of collagen–proteoglycan solid matrix per unit volume of the specimen [31]. Negatively charged contrast agent ($Gd\text{-}DTPA^{2-}$) penetrates dominantly to the areas with low GAG concentration; therefore, the strong negative correlation of *I*/*Eq* and GAG content found in this study is in good agreement with this fact. Estimation of biomechanical properties of articular cartilage by MRI has been previously investigated in several studies [30,45]. Nieminen et al. found, in bovine cartilages, that up to 87% of the variation in biomechanical parameters can be explained by MRI parameters (in

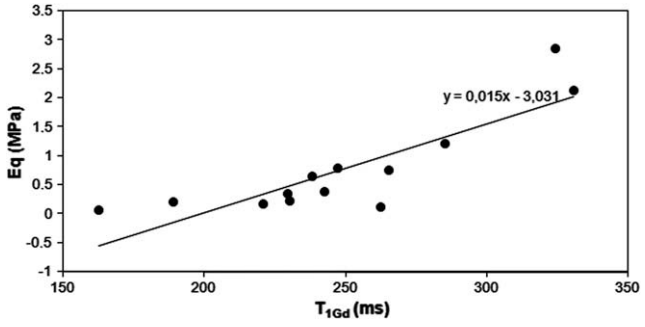

Fig. 3. Correlation plot between bulk T_{1Gd} vs equilibrium modulus (*Eq*) in degenerated articular cartilage; correlation coefficient r = 0.8095; N = 13. The variables are related by the regression equation, $Eq = 0.015 \times T_{1Gd} - 3.031$.

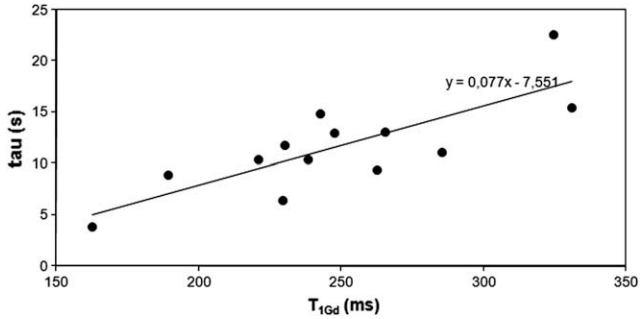

Fig. 4. Correlation plot between bulk T_{1Gd} vs tissue relaxation time τ in articular cartilage; correlation coefficient $r = -0.8469$; $N = 13$. The variables are related by the regression equation, $\tau = -0.077 \times T_{1Gd} - 7.551$.

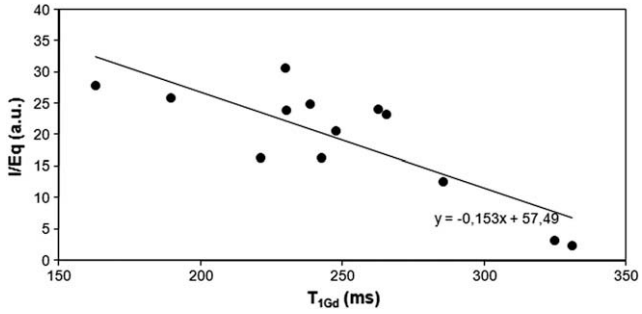

Fig. 5. Correlation plot between bulk T_{1Gd} vs *I*/*Eq* ratio; correlation coefficient $r = -0.8441$; $N = 13$. The variables are related by the regression equation, $I/Eq = -0.153 \times T_{1Gd} + 57.49$.

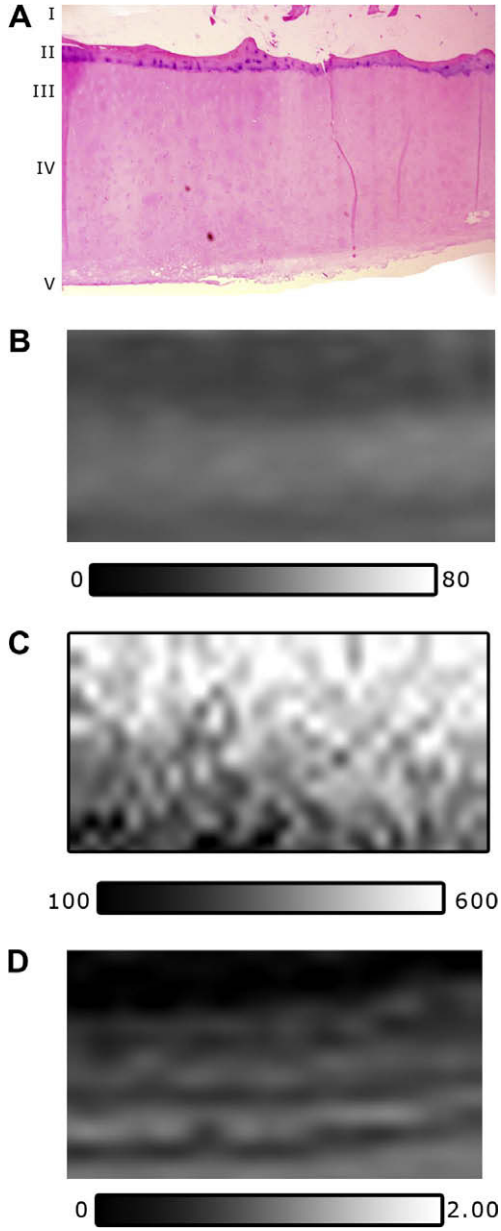

Fig. 6. Mild OA: cartilage surface (V) with fibrillation; transitional (IV) and deep (III) zones are intact, as well as cartilage-bone interface (II) and subchondral bone (I). (A) histological slice, H&E, magnification ×40; (B) T_2 maps with obvious stratification (values in ms); (C) T_{1Gd} map, related to GAG content, which decreases with depth relative to the cartilage surface (values in ms); (D) ADC map with no apparent zonal differentiation (values in $\times 10^{-3}$ mm^2/s).

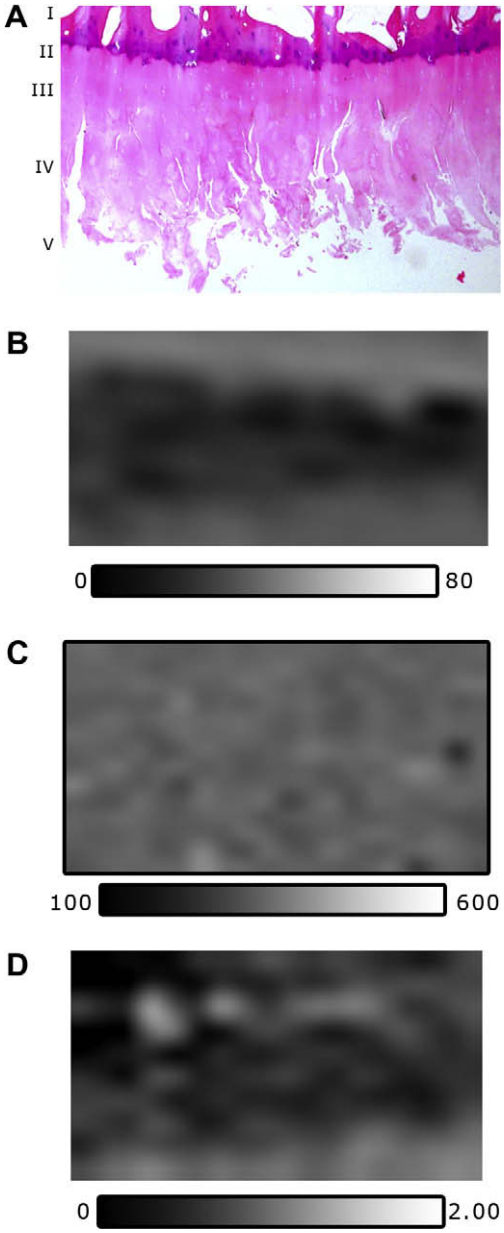

Fig. 7. Advanced OA: damage with deep fissures and clefts leading to loss of cartilage. (A) histological slice, H&E, magnification × 40; (B) T2 map with corrupted stratification (values in ms); (C) lower GAG content on T_{1Gd} map with less apparent decrease of GAG in the direction of the deep tissue (values in ms); (D) ADC map with no apparent zonal differentiation (values in $\times 10^{-3}$ mm^2/s).

particular T_{1Gd}) [30]. Setton et al. used an experimental model of joint degeneration to reveal that, in human cartilage with OA, tensile, compressive, and shear behaviors are dramatically altered [46]. The laboratory biochemical analysis of PG and collagen content in articular cartilage (used as a gold standard) can precisely determine the correlation of these components with biomechanical properties. In previously published studies good correlation was found between PG and collagen content and many biomechanical parameters (equilibrium and dynamic modulus, hydraulic permeability, dynamic stiffness, streaming potential, or electrokinetic coupling coefficient) using biochemical analysis [47,48]. Correlations calculated in our study (in particular T_{1Gd} vs *Eq* and T_2 vs *Eq*) are slightly higher than those presented in detailed biochemical analysis [47]. This discrepancy can be explained by relatively low number of specimens in our study; thus, future studies will be aimed at increasing the number of samples and proving the results.

dGEMRIC has been shown to have the potential to quantify the distribution of GAG across the cartilage tissue [13,14]. In the early stage of osteoarthritis, a loss of GAG is typical and progresses with advanced disease. Although the measurements in this study were performed on cartilage explants, dGEMRIC was proven to work in the same way in *in vivo* conditions [13]. One must note, however, that macromolecular content can influence the relaxivity of Gd-DTPA^{2-} [49], and this must be considered when interpreting the results.

Since regional variations in collagen fibril orientation determine the T_2 heterogeneity of articular cartilage, in healthy cartilage tissue, a typical profile shows a decreasing trend for T_2 from the

Table 1
Correlation coefficients between MR and biomechanical parameters.

	Bulk	Superficial	Middle	Deep
T_{1Gd} vs I	−0.4136	−0.3986	−0.2738	−0.4319
T_{1Gd} vs Eq	**0.8095**	**0.8072**	**0.9031**	0.7568
T_{1Gd} vs I/Eq	**−0.8441**	**−0.9491**	**−0.9445**	**−0.8011**
T_{1Gd} vs τ	**0.8469**	**0.8610**	**0.9243**	**0.9053**
[Gd-DTPA] vs I	0.1577	0.1130	0.1819	0.2109
[Gd-DTPA] vs Eq	**−0.8732**	−0.6599	**−0.9466**	−0.1282
[Gd-DTPA] vs I/Eq	**0.9320**	**0.8219**	**0.9638**	−0.3707
[Gd-DTPA] vs τ	**−0.8351**	−0.5739	**−0.9621**	−0.1440
T_2 vs I	0.1197	−0.2597	0.1554	0.0577
T_2 vs Eq	0.4717	0.3981	0.4842	0.3197
T_2 vs I/Eq	−0.4647	−0.3017	−0.4950	−0.5091
T_2 vs τ	0.4085	0.4116	0.2747	0.3472
ADC vs I	0.3757	−0.1834	0.3406	0.1608
ADC vs Eq	−0.5236	−0.6427	0.0596	−0.3943
ADC vs I/Eq	0.2969	0.5567	−0.3282	0.5938
ADC vs τ	−0.3975	−0.7262	0.0954	−0.3338

T_{1Gd}: longitudinal relaxation time after contrast addition; T_2: transversal relaxation time; ADC: apparent diffusion coefficient; I: instantaneous modulus (MPa); Eq: equilibrium modulus (MPa); τ: relaxation time (s). The highest correlations are in bold; more detailed description can be found within the text.

Table 2
Calculated MR parameters of degenerated articular cartilage in different zones.

CZ/MR	T_1 [ms]	T_{1Gd} [ms]	[Gd-DTPA] [mM]	T_2 [ms]	ADC [10^{-3} mm^2/s]
Bulk	530 ± 60	178 ± 51	1.2 ± 0.4	28 ± 8	1.00 ± 0.14
Superficial	620 ± 70	105 ± 13	1.3 ± 0.3	26 ± 7	1.21 ± 0.2
Middle	528 ± 86	166 ± 51	1.3 ± 0.2	41 ± 14	0.98 ± 0.08
Deep	370 ± 50	330 ± 40	0.11 ± 0.05	23 ± 6	0.86 ± 0.12

CZ: cartilage zone; MR: biochemical parameters obtained from MR.

superficial layer down to the deep layer [50–52]. In this study, low correlation between T_2 and selected biomechanical properties was recorded in bulk and in zonal separation ($r_{max} = -0.5091$ in deep zone). In the inter-species study by Nissi et al., a complex relationship between T_2 and the mechanical properties of cartilage tissue was observed [45]. They concluded that cartilage composition and structure, as reflected by MRI, has a complicated relationship with the characteristics of mechanical performance. However, Lammentausta et al. demonstrated the feasibility of quantitative MRI, particularly T_2 mapping, to reflect the mechanical properties of native human patellar cartilage at field strengths of 1.5 T and 9.4 T [28]. The results of our study suggest that prediction of biomechanical parameters for degenerated articular cartilage may not be simply extrapolated from assessment of native tissue. T_2 values were measured in the presence of Gd-DTPA^{2-}, however, this paramagnetic contrast agent does not influence T_2 values at low equilibrated concentrations [53]. As T_2 is related primarily to the orientation of collagen fibers, one can expect that T_2 would better correlate with biomechanical parameters not measured in this study, such as modulus of rigidity (shear modulus) or tensile strength.

Diffusion-weighted imaging (DWI) of articular cartilage has been demonstrated *in vitro* to be sensitive to early cartilage degradation [50,54]. ADC decreases at long diffusion times, indicative of the water molecules being restricted by cartilage components. At the diffusion times typically used, this restriction is related to the collagen network in cartilage [24]. Similar to T_2, correlation coefficients between ADCs and mechanical properties were low ($r_{max} = 0.5938$ in deep layer). Since ADC is an anisotropic measure, and, in this study, DWI was not performed in three dimensions but was only obtained in the read-out direction, this limits its value to some extent. On the other hand, the diffusion measured only in one direction may also provide useful information about the status of cartilage components.

It is important to mention that correlation of T_2 and ADC with mechanical parameters is limited in our study by the selection of parameters (Eq, I, and τ).

Using higher MR image resolution would help with defining particular cartilage zones in the evaluation process, but also would double the measurement time. Fortunately, human knee cartilage is thick enough for evaluation with the resolution used in this study. In any case, bulk values of MR parameters should be also evaluated, because, although the cartilage thickness was sufficient, partial volume effects may cause questionable inaccuracies when selecting particular zones. Moreover, in advanced stages of degeneration, the superficial zone of articular cartilage may be eroded down to the middle zone, or in advanced cases even to the deep zone. Nevertheless, the selection of cartilage used for explant preparation was visually controlled; therefore, only relatively intact cartilage with preserved thickness was included in the study.

The specimens used in this study were harvested from lateral femoral condyles only. In order to validate the findings of this study, more anatomical locations should be evaluated since biomechanical properties of articular cartilage and their relation to MR parameters may vary across topographic and anatomical location [28].

The assessed specimens of articular cartilage were stored frozen before examination. Extremely low temperatures may cause structural and compositional changes in articular cartilage [55], with a potential impact on the biomechanical properties of the tissue. Since we stored the samples at mild temperatures only (−18 °C), the effect on the observed MR parameters may be negligible. Moreover, Kiefer et al. showed that cryopreservation has a minimal influence on the mechanical parameters of articular cartilage [56].

Another limitation of this study could be the temperature of measured samples. Since the cartilage explants were placed in a micro-imaging system that needs to be cooled to 12 °C, the explants were far below body temperature. On the other hand, Nelson et al. showed a relatively low T_2 dependence on temperature [57]. They showed, as well, that the temperature dependence coefficient (TDC) of T_1 is relatively high, but since the temperature along all measurements was kept constant, its influence on particular correlations is small. A calculation of contrast agent concentration can be also considered as a potential limitation. Higher proton relaxivity is reached by increasing the rotational correlation time which is temperature dependent. Although the difference between reduced relaxation rate (T_{1r}) at 12 °C and 37 °C is relatively low [58], potential bias of calculated [Gd-DTPA] must be taken in account while interpreting the results.

In conclusion, the results of this study show that certain (but not all) MR parameters allow one to non-invasively estimate some of the variability of the biomechanical properties of articular cartilage.

Acknowledgments

The authors thank Dr. Reinhard Fuiko for providing cartilage specimens. Funding for this study was provided by the Austrian Science Fund (FWF) FWF—Project P-18110-B15 and Slovak Scientific Grant Agency VEGA 2/0142/08.

References

[1] W.C. Hayes, G. Herrmann, L.F. Mockros, L.M. Keer, Mathematical-analysis for indentation tests of articular-cartilage, Journal of Biomechanics 5 (1972) 541–551.
[2] J.R. Parsons, J. Black, The viscoelastic shear behavior of normal rabbit articular cartilage, Journal of Biomechanics 10 (1977) 21–29.

[3] V.C. Mow, W.M. Lai, Mechanics of animal joints, Annual Review of Fluid Mechanics 11 (1979) 247–288.
[4] V.C. Mow, W.M. Lai, Recent developments in synovial joint biomechanics, Siam Review 22 (1980) 275–317.
[5] M.S. Laasanen, J. Toyras, R.K. Korhonen, J. Rieppo, S. Saarakkala, M.T. Nieminen, J. Hirvonen, J.S. Jurvelin, Biomechanical properties of knee articular cartilage, Biorheology 40 (2003) 133–140.
[6] R.C. Appleyard, P. Ghosh, M.V. Swain, Biomechanical histological and immunohistological studies of patellar cartilage in an ovine model of osteoarthritis induced by lateral meniscectomy, Osteoarthritis and Cartilage 7 (1999) 281–294.
[7] G.E. Kempson, H. Muir, C. Pollard, M. Tuke, Tensile properties of cartilage of human femoral condyles related to content of collagen and glycosaminoglycans, Biochimica Et Biophysica Acta 297 (1973) 456–472.
[8] J.C. Bucklandwright, Quantitative radiography of osteoarthritis, Annals of the Rheumatic Diseases 53 (1994) 268–275.
[9] B.R. Daenen, M.A. Ferrara, S. Marcelis, R.F. Dondelinger, Evaluation of patellar cartilage surface lesions: comparison of CT arthrography and fat-suppressed FLASH 3D MR imaging, European Radiology 8 (1998) 981–985.
[10] W. Grassi, G. Lamanna, A. Farina, C. Cervini, Sonographic imaging of normal and osteoarthritic cartilage, Seminars in Arthritis and Rheumatism 28 (1999) 398–403.
[11] M.T. Nieminen, J. Toyras, J. Rieppo, J.M. Hakumaki, J. Silvennoinen, H.J. Helminen, J.S. Jurvelin, Quantitative MR microscopy of enzymatically degraded articular cartilage, Magnetic Resonance in Medicine 43 (2000) 676–681.
[12] F. Eckstein, L. Heudorfer, S.C. Faber, R. Burgkart, K.H. Englmeier, M. Reiser, Long-term and resegmentation precision of quantitative cartilage MR imaging (qMRI), Osteoarthritis and Cartilage 10 (2002) 922–928.
[13] D. Burstein, J. Velyvis, K.T. Scott, K.W. Stock, Y.J. Kim, D. Jaramillo, R.D. Boutin, M.L. Gray, Protocol issues for delayed Gd(DTPA)(2-)-enhanced MRI: (dGEMRIC) for clinical evaluation of articular cartilage, Magnetic Resonance in Medicine 45 (2001) 36–41.
[14] S. Trattnig, S. Marlovits, S. Gebetsroither, P. Szomolanyi, G.H. Welsch, E. Salomonowitz, A. Watanabe, M. Deimling, T.C. Mamisch, Three-dimensional delayed gadolinium-enhanced MRI of cartilage (dGEMRIC) for in vivo evaluation of reparative cartilage after matrix-associated autologous chondrocyte transplantation at 3.0T: preliminary results, Journal of Magnetic Resonance Imaging 26 (2007) 974–982.
[15] Y. Xia, Magic-angle effect in magnetic resonance imaging of articular cartilage - A review, Investigative Radiology 35 (2000) 602–621.
[16] S. Lusse, H. Claassen, T. Gehrke, J. Hassenpflug, M. Schunke, M. Heller, C.C. Gluer, Evaluation of water content by spatially resolved transverse relaxation times of human articular cartilage, Magnetic Resonance Imaging 18 (2000) 423–430.
[17] M. Uhl, C. Ihling, K.H. Allmann, J. Laubenberger, U. Tauer, C.P. Adler, M. Langer, Human articular cartilage: in vitro correlation of MRI and histologic findings, European Radiology 8 (1998) 1123–1129.
[18] G.H. Welsch, T.C. Mamisch, S.E. Domayer, R. Dorotka, F. Kutscha-Lissberg, S. Marlovits, L.M. White, S. Trattnig, Cartilage T2 assessment at 3-T MR imaging: in vivo differentiation of normal hyaline cartilage from reparative tissue after two cartilage repair procedures - initial experience, Radiology 247 (2008) 154–161.
[19] M.A. Bredella, P.F.J. Tirman, C.G. Peterfy, M. Zarlingo, J.F. Feller, F.W. Bost, J.P. Belzer, T.K. Wischer, H.K. Genant, Accuracy of T2-weighted fast spin-echo MR imaging with fat saturation in detecting cartilage defects in the knee: comparison with arthroscopy in 130 patients, American Journal of Roentgenology 172 (1999) 1073–1080.
[20] J.E. Tanner, Pulsed field gradients for NMR spin-echo diffusion measurements, Review of Scientific Instruments 36 (1965) 1086–1087.
[21] T.C. Mamisch, M.I. Menzel, G.H. Welsch, B. Bittersohl, E. Salomonowitz, P. Szomolanyi, J. Kordelle, S. Marlovits, S. Trattnig, Steady-state diffusion imaging for MR in-vivo evaluation of reparative cartilage after matrix-associated autologous chondrocyte transplantation at 3 tesla - Preliminary results, European Journal of Radiology 65 (2008) 72–79.
[22] V. Mlynarik, I. Sulzbacher, R. Fuiko, M. Bittsansky, S. Trattnig, Apparent diffusion constant as an indicator of early degenerative disease in articular cartilage, Radiology 225 (2002) 329–330.
[23] V. Mlynarik, I. Sulzbacher, M. Bittsansky, R. Fuiko, S. Trattnig, Investigation of apparent diffusion constant as an indicator of early degenerative disease in articular cartilage, Journal of Magnetic Resonance Imaging 17 (2003) 440–444.
[24] D. Burstein, M.L. Gray, A.L. Hartman, R. Gipe, B.D. Foy, Diffusion of small solutes in cartilage as measured by nuclear-magnetic-resonance (NMR) spectroscopy and imaging, Journal of Orthopaedic Research 11 (1993) 465–478.
[25] J. Rieppo, J. Toyras, M.T. Nieminen, V. Kovanen, M.M. Hyttinen, R.K. Korhonen, J.S. Jurvelin, H.J. Helminen, Structure-function relationships in enzymatically modified articular cartilage, Cells Tissues Organs 175 (2003) 121–132.
[26] L.P. Li, M.D. Bushmann, A. Shirazi-Adl, Alterations in mechanical behavior of articular cartilage due to loss of material inhomogeneity, Archives of Physiology and Biochemistry 108 (2000) 172.
[27] R.U. Kleemann, D. Krocker, A. Cedraro, J. Tuischer, G.N. Duda, Altered cartilage mechanics and histology in knee osteoarthritis: relation to clinical assessment (ICRS Grade), Osteoarthritis and Cartilage 13 (2005) 958–963.
[28] E. Lammentausta, P. Kiviranta, M.J. Nissi, M.S. Laasanen, I. Kiviranta, M.T. Nieminen, J.S. Jurvelin, T-2 relaxation time and delayed gadolinium-enhanced MRI of cartilage (dGEMRIC) of human patellar cartilage at 1.5 T and 9.4 T: relationships with tissue mechanical properties, Journal of Orthopaedic Research 24 (2006) 366–374.
[29] T. Lyyra, J. Jurvelin, P. Pitkanen, U. Vaatainen, I. Kiviranta, Indentation instrument for the measurement of cartilage stiffness under arthroscopic control, Medical Engineering and Physics 17 (1995) 395–399.
[30] M.T. Nieminen, J. Toyras, M.S. Laasanen, J. Silvennoinen, H.J. Helminen, J.S. Jurvelin, Prediction of biomechanical properties of articular cartilage with quantitative magnetic resonance imaging, Journal of Biomechanics 37 (2004) 321–328.
[31] C.G. Armstrong, V.C. Mow, Variations in the intrinsic mechanical proterties of human articular-cartilage with age, degeneration, and water-content, Journal of Bone and Joint Surgery. American volume 64 (1982) 88–94.
[32] M. Rohrer, H. Bauer, J. Mintorovitch, M. Requardt, H.J. Weinmann, Comparison of magnetic properties of MRI contrast media solutions at different magnetic field strengths, Investigative Radiology 40 (2005) 715–724.
[33] G.M. Bydder, M.A. Rutherford, J.V. Hajnal, How to perform diffusion-weighted imaging, Childs Nervous System 17 (2001) 195–201.
[34] J.M. Modl, L.A. Sether, V.M. Haughton, J.B. Kneeland, Articular-cartilage - correlation of histologic zones with signal intensity at MR imaging, Radiology 181 (1991) 853–855.
[35] H. Jin, J.L. Lewis, Determination of Poisson's ratio of articular cartilage by indentation using different-sized indenters, Journal of Biomechanical Engineering-Transactions of the Asme 126 (2004) 138–145.
[36] J. Jurvelin, I. Kiviranta, M. Tammi, H.J. Helminen, Effect of physical exercise on indentation stiffness of articular-cartilage in the canine knee, International Journal of Sports Medicine 7 (1986) 106–110.
[37] V.C. Mow, M.C. Gibbs, W.M. Lai, W.B. Zhu, K.A. Athanasiou, Biphasic indentation of articular-cartilage.2. A numerical algorithm and an experimental-study, Journal of Biomechanics 22 (1989) 853–861.
[38] H. Buckle, The science of hardness testing and its research applications, in: J.W. Westbrook, H. Conrad (Eds.), American Society for Materials, Metals Park, OH, 1973, p. 453.
[39] I. Manika, J. Maniks, Effect of substrate hardness and film structure on indentation depth criteria for film hardness testing, Journal of Physics D-Applied Physics 41 (2008) 1–6.
[40] J.A. Buckwalter, V.C. Mow, A. Ratcliffe, Restoration of injured or degenerated articular cartilage, The Journal of the American Academy of Orthopaedic Surgeons 2 (1994) 192–201.
[41] M. LaBerge, in: Mechanical Testing of Cartilage Animal Models in Orthopaedic Research, CRC Press, Boca Raton, FL, 1999, pp. 165–174.
[42] J.S. Jurvelin, M.D. Buschmann, E.B. Hunziker, Optical and mechanical determination of Poisson's ratio of adult bovine humeral articular cartilage, Journal of Biomechanics 30 (1997) 235–241.
[43] M. Stolz, R. Raiteri, A.U. Daniels, M.R. VanLandingham, W. Baschong, U. Aebi, Dynamic elastic modulus of porcine articular cartilage determined at two different levels of tissue organization by indentation-type atomic force microscopy, Biophysical Journal 86 (2004) 3269–3283.
[44] R.L. Mauck, M.A. Soltz, C.C.B. Wang, D.D. Wong, P.H.G. Chao, W.B. Valhmu, C.T. Hung, G.A. Ateshian, Functional tissue engineering of articular cartilage through dynamic loading of chondrocyte-seeded agarose gels, Journal of Biomechanical Engineering-Transactions of the Asme 122 (2000) 252–260.
[45] M.J. Nissi, J. Rieppo, J. Toyras, M.S. Laasanen, I. Kiviranta, M.T. Nieminen, J.S. Jurvelin, Estimation of mechanical properties of articular cartilage with MRI - dGEMRIC, T-2 and T-1 imaging in different species with variable stages of maturation, Osteoarthritis and Cartilage 15 (2007) 1141–1148.
[46] L.A. Setton, D.M. Elliott, V.C. Mow, Altered mechanics of cartilage with osteoarthritis: human osteoarthritis and an experimental model of joint degeneration, Osteoarthritis and Cartilage 7 (1999) 2–14.
[47] J.S. Wayne, K.A. Kraft, K.J. Shields, C. Yin, J.R. Owen, D.G. Disler, MR imaging of normal and matrix-depleted cartilage: correlation with biomechanical function and biochemical composition, Radiology 228 (2003) 493–499.
[48] S. Treppo, H. Koepp, E.C. Quan, A.A. Cole, K.E. Kuettner, A.J. Grodzinsky, Comparison of biomechanical and biochemical properties of cartilage from human knee and ankle pairs, Journal of Orthopaedic Research 18 (2000) 739–748.
[49] G.J. Stanisz, R.M. Henkelman, Gd-DTPA relaxivity depends on macromolecular content, Magnetic Resonance in Medicine 44 (2000) 665–667.
[50] Y. Xia, T. Farquhar, N. BurtonWurster, G. Lust, Origin of cartilage laminae in MRI, Jmri-Journal of Magnetic Resonance Imaging 7 (1997) 887–894.
[51] V. Mlynarik, A. Degrassi, R. Toffanin, F. Vittur, M. Cova, R.S. PozziMucelli, Investigation of laminar appearance of articular cartilage by means of magnetic resonance microscopy, Magnetic Resonance Imaging 14 (1996) 435–442.
[52] J. Rubenstein, M. Recht, D.G. Disler, J. Kim, R.M. Henkelman, Laminar structures on MR images of articular cartilage, Radiology 204 (1997) 15–16.
[53] M.T. Nieminen, N.M. Menezes, A. Williams, D. Burstein, T-2 of articular cartilage in the presence of Gd-DTPA(2-), Magnetic Resonance in Medicine 51 (2004) 1147–1152.
[54] J.B. Kneeland, MRI probes Biophysical structure of cartilage, Diagn Imaging (San Franc) 18 (1996) 36–40.
[55] H. Notzli, J. Clark, Deformation of loaded articular cartilage prepared for scanning electron microscopy with rapid freezing and freeze-substitution fixation, Journal of Orthopaedic Research 15 (1997) 76–86.

[56] G.N. Kiefer, K. Sundby, D. Mcallister, N.G. Shrive, C.B. Frank, T. Lam, N.S. Schachar, The effect of cryopreservation on the biomechanical behavior of bovine articular-cartilage, Journal of Orthopaedic Research 7 (1989) 494–501.
[57] T.R. Nelson, S.M. Tung, Temperature-dependence of proton relaxation-times invitro, Magnetic Resonance Imaging 5 (1987) 189–199.
[58] E.E. Toth, S. Vauthey, D. Pubanz, A.E. Merbach, Water exchange and rotational dynamics of the dimeric gadolinium(III) complex [BO{Gd(DO3A)(H(2)O)}(2)]: a variable-temperature and -pressure (17)O NMR study(1), Inorganic Chemistry 35 (1996) 3375–3379.